Fabrication of thin-film neural implants

Authors: Poppy Oldroyd[1]*, Santiago Velasco-Bosom[1]*, Sophia Lee Bidinger[1]*, Tawfique Hasan[1], Alexander J. Boys[2,3]c, George G. Malliaras[1]c
*co-first author
cco-corresponding

[1] Electrical Engineering Division, Department of Engineering, University of Cambridge, CB3 0FA, United Kingdom

[2] Department of Chemical Engineering and Biotechnology, University of Cambridge, CB3 0AS, United Kingdom

[3] Thayer School of Engineering, Dartmouth College, Hanover, NH 03755, USA

Abstract

Bioelectronic medicine, which involves the delivery of electrical stimulation with implantable electrodes, shows great promise in the treatment of neurological conditions. However current hand-made devices are bulky, invasive, and lack specificity. Thin-film neurotechnology devices can overcome these disadvantages. With a typical thickness in the range of tens of micrometers, they demonstrate high conformability, stretchability, and are minimally invasive. These devices can be fabricated using traditional lithography techniques. Despite their potential, variability and unreliability in fabrication hinder progress. Here, we detail a fabrication method for thin-film PEDOT:PSS electrodes and organic electrochemical transistors. The use of organic materials makes these devices particularly well-suited for bioelectronic medicine applications as they show superior mechanical and electrical matching of biological tissues compared to devices made of inorganic materials. This method details the entirety of the process, including mask design, fabrication through three photolithography steps, integration with larger scale electronics, implantation procedures, and the expected electrical characterization metrics. The nanofabrication protocol requires at least 3 days and is suitable for those familiar with lithographic fabrication procedures. The surgery requires up to 10 hours and is suitable for those familiar with in vivo implantation procedures.

Introduction

Bioelectronic implants have revolutionized medical research and treatment, enabling the study of the human brain and offering therapeutic solutions for neurological conditions affecting over 1.3 billion people worldwide[1]. Originating from Luigi Galvani's pioneering experiments in the 18th century, the evolution of neural implants has led to the creation of sophisticated devices capable of restoring function across various medical conditions. A prominent example is deep brain stimulation, a notable achievement in this field, which has proven effective in managing motor symptoms in

patients with movement disorders including Parkinson's disease[2]. Spinal cord stimulators have played a pivotal role in enhancing chronic pain management[3] and have shown promise in restoring limb function by facilitating direct brain-to-muscle communication[4]. Additionally, responsive neurostimulation devices have demonstrated success in reducing the number of epileptic seizures through closed-loop designs[5].

Despite these advancements, challenges persist due to the use of both large-scale processes and manual production for these implants [6]. The resulting implants are bulky, exhibit poor conformability to organ surfaces, eliciting significant foreign body response that diminishes treatment efficacy[6–8]. These hurdles currently impede the widespread deployment of these devices to benefit a broader patient population. Such translational challenges have spurred the development of thin-film neural implants[9], offering distinct advantages over past implants and facilitating further progress in medical applications. Thin-film neural implants, with a typical thickness of the order of tens of micrometers, can demonstrate high conformability, stretchability, and be made minimally invasive[10–16]. These characteristics notably reduce the foreign body response and, in the form of 2D microelectrode arrays (MEAs), offer hundreds or thousands of μm-sized electrodes, ensuring high spatiotemporal resolution for recording and stimulation capabilities across large tissue areas[9].

The fabrication process takes inspiration from the semiconductor industry using microfabrication of integrated circuits. However, it is distinct in its use of organic materials instead of silicon-based materials. Khodagholy, *et al.* demonstrated two pioneering works in this field. First was the demonstration of high signal-to-noise ratio *in vivo* brain recordings using organic electrochemical transistors [17]. Second was the development of Neurogrid [9]. The protocol detailed here is based on the same device architecture, consisting of parylene-C, gold, and PEDOT:PSS, which has since been used in many other studies. Notable modifications to the protocol here compared to the Neurogrid and *in vivo* OECTs include adjustments in photoresists to enhance the reproducibility and resolution of the photolithography steps and introduction of procedures for bonding implants to a flexible cable using anisotropic conductive film, facilitating easier manipulation during implantation.

Many research institutes and universities possess the means to make these types of devices but lack the knowledge required to transfer the standard methodologies for producing stiff, silicon-based devices into production of flexible implantable bioelectronics. In order to elucidate the full manufacturing process for widespread accessibility to the versatile implant approach, we have provided an in-depth protocol including main errors, mitigation measures, and expected electrochemical characterization results. In addition, we have provided detailed implantation protocols for variety of *in vivo* applications.

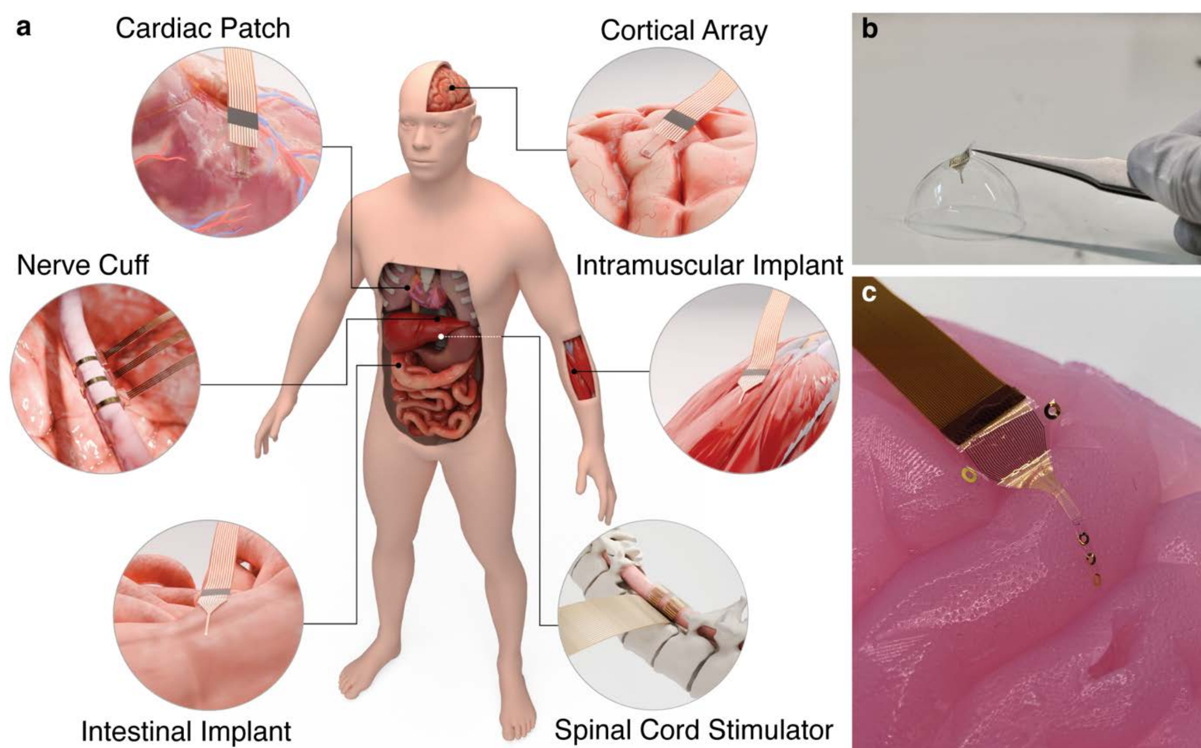

Fig.1: Overview of thin-film neural implants and their applications
a, Along with many demonstrated applications of thin-film neural implants in and on the brain, similar devices have been applied throughout the body. For example, they have been demonstrated on muscles for electromyography (EMG), on the spinal cord towards treating spinal cord injury (SCI), on the intestines to study gut electrophysiology, around peripheral nerves to bypass injury, and on the heart for electrocardiography (ECG). **b**, Thin-film neural implant placed on a soap bubble showcases soft contact of these devices onto fragile structures. **c**, Thin-film neural implant showing conformability on an agarose brain model.

Applications of the method:
Thin-film fabrication on flexible substrates is a promising approach that has opened up new avenues for neural implant development (Fig. 1a)[18,19]. Traditionally difficult to interface, dynamic and mobile tissues like those found in the viscera are now accessible, where thin-film implants have been shown to provide effective modulation of gut and intestinal function, offering relief for conditions like irritable bowel syndrome, gastroparesis, and inflammatory bowel disease[20,21]. The historically utilized stiff bioelectronic devices have been unable to interface with the intricate and fragile nerves of the peripheral nervous system, whereas thin-film neural implants (Fig. 1b,c) have produced high quality sub-nerve resolution recordings[22]. These implants have also been combined with tissue engineered and cellular modalities for improved interfacing[23,24]. Additional functionality, like chemical sensing, can also be incorporated into thin-film neural implants by integrating organic semiconductor materials [25]. Organic electrochemical transistors (OECTs) incorporated into these

implants have demonstrated success in sensing various biomolecules, including neurotransmitters like dopamine and serotonin[26], thereby aiding in the understanding and treatment of neurological conditions. Additionally, OECTs detect biomarkers such as glucose for diabetes management[27], pH sensors monitor acid-base imbalances[28], and ion sensors detect concentrations of sodium, potassium, and calcium[29], providing real-time data for enhanced physiological understanding and personalized treatments.

The primary audience of this protocol is researchers, engineers, and scientists engaged in the development of thin-film devices intended for bi-directional monitoring and stimulation of the brain and various physiological systems throughout the body. These researchers include fundamental neuroscientists investigating neural activity to address unexplored questions, as well as applied biomedical engineers developing interventions for currently untreatable diseases. Materials researchers such as those looking at transport within polymers will be able to use this protocol to fabricate OECT's to test their materials. Electrical engineers will also find this protocol useful for building devices for bi-directional circuits and recording systems. Additionally, the protocol holds relevance for clinical researchers investigating potential medical applications.

Comparison with other methods:

In the domain of thin-film neurotechnology devices, certain choices and methodologies have emerged as preferred strategies for fabrication. Polymer-based substrate and encapsulation materials, such as parylene-C (PaC)[9] and poly(imide) (PI)[30], have garnered widespread acceptance due to their exceptional biocompatibility[31] and mechanical properties[32]. In this protocol a stack of PaC/Ti/Au/PaC is used, however other thin-film stacks are available. One common stack is PI/Pt/PI [33], due to the processing of PI, these devices tend to be slightly thicker around 11 µm compared to the 4 µm thickness of the devices in this protocol. Additionally, comparative studies demonstrated that PaC outperforms polyimide as an encapsulation material for neural implants, exhibiting enhanced long-term stability in saline environments [34]. In this protocol paper, we use PaC, chosen for its electrical insulation properties, conformability, thickness, and optical transparency.

Micron-scale tracks and features are patterned using photolithography, with nanometer-thick metal deposition using thermal or e-beam evaporation. Traditionally, platinum (Pt) [35] or gold (Au) [36] with an adhesion promoter, commonly chromium (Cr) or titanium (Ti), to the polymer substrate are utilized. This protocol employs 100 nm Au with 10 nm Ti. Au was selected over Pt as the electrode layer due to lower material cost and lower power needed to evaporate, providing increased ease-of-manufacturing. Ti was chosen as the adhesion promoter over Cr due to its general improvement in biocompatibility versus Cr. Further information for a relative comparison between these materials as an adhesion layer is well-outlined in other

reviews [37]. Other common alternative methods relate to metal patterning using a lift-off versus a wet-etching procedure, the use of different etch masks, such a photoresist versus a metallic etch-mask, as well as different types of aligners for photolithography, mask versus maskless aligners. For our protocol, we utilize a lift-off method for patterning, photoresist etch masks, and a mask aligner. However, the exact protocol will vary per the available techniques and equipment in any particular cleanroom, as is noted below.

Historically, this stage would have marked the conclusion of thin-film implant fabrication. However, a recent trend involves applying an additional layer to coat the metal electrodes, enhancing their electrical properties while helping to prevent mechanical failure[38,39]. Common materials for this purpose are conductive polymers[9] and carbon-based structures[40]. In this protocol, the conductive polymer poly(ethylene dioxythiophene):poly(styrene sulfonate) (PEDOT:PSS) is chosen for its solution-processing capabilities and the reduction it affords in impedance at the interface. The coating layer can be patterned via photolithography and RIE [41], and through the use of a sacrificial layer and subsequent peel-off to leave behind the desired pattern. In this protocol, the coating layer is patterned using this sacrificial layer technique, selected as the least aggressive method for PEDOT:PSS processing, minimizing the risk of exposing it to ions and other chemicals that could impact its chemical composition.

Benefits of the protocol:

The key advantages of this technique are that it enables the development of micron scale thin-film devices that minimize implantation damage. All of the fabrication techniques are cleanroom compatible and therefore are reproducible and reliable. Moreover, the mask design can be tailored to application making its potential applications vast.

Limitations of the protocol:

Although this approach is highly flexible, it is mostly limited by the high number of steps required, which makes it difficult to scale-up to industry-level production. Additionally the specialized equipment needed to fabricate these devices means the protocol has to be carried out in a cleanroom facility. It is important to acknowledge that cleanroom equipment can vary, which would require some retooling of the technique to cleanroom specific devices.

Overview of the Procedure:

The process involves several key steps including substrate deposition, metal deposition, insulation, PEDOT:PSS coating, etching, and bonding. The outline of the main processes is as follows:

Substrate Deposition: The process commences with the deposition of a polymer-based substrate (PaC) onto a silicon wafer (Fig. 2a).

Metal Deposition and Patterning: Thin-film metal components (Au, Ti) undergo patterning through photolithography and subsequent deposition via e-beam evaporation (Fig. 2b).

Insulation Deposition and Patterning: An insulation layer of PaC is deposited through CVD. The outline of the devices is etched away to allow the devices to be released from the underlying silicon wafer (Fig. 2c). This is followed by the opening of the active areas of the device for biological interaction. The etching processes are usually performed using reactive ion etching (RIE) to precisely pattern the electrode- or transistor-regions for electrolyte and biological medium exposure during application.

PEDOT:PSS Deposition and Patterning: Initially, a sacrificial layer of PaC is deposited, succeeded by the application of a conductive polymer (PEDOT:PSS) coating aimed at enhancing electrical properties and mitigating mechanical failure (Fig. 2d).

Peel-Off: Peel-off technique of sacrificial layer to leave behind the intended pattern of PEDOT:PSS for electrode coatings or transistor channels (Fig. 2e).

Bonding: Following removal from the wafer, devices are bonded to flexible cables with anisotropic conductive film (ACF).

Pre-operative Preparation (Mouse or Rat): Pre-operative procedure for inducing a mouse or rat for surgery.

Electrocorticography Array Placement: Overview of method for electrocorticography array placement.

Nerve Cuff Placement: Overview of method for nerve cuff placement.

Intramuscular Implant Placement: Overview of method for intramuscular device placement.

Spinal Array Placement: Overview of method for spinal array placement.

Post-operative Recovery: Post-operative recovery procedure.

Recording / Stimulation & Post-processing (in brief): Brief explanation of relevant mechanisms for interfacing with a microfabricated, thin-film device post-implantation.

Additional Steps Suggested:

Mask Design: Optimal mask design is crucial for accurate patterning, involving strategic distribution of devices on the wafer and multiple lithography steps.

Characterization: The fabricated devices are characterized for their electrical properties using techniques such as electrochemical impedance spectroscopy (EIS) for electrodes and measuring transfer and output characteristics for OECTs (Organic Electrochemical Transistors). Metrology measurements are provided for a discussion around the reproducibility of the protocol.

Troubleshooting: Common issues during fabrication are discussed, along with methods to overcome them.

Potential Applications: The protocol outlines potential applications for these thin-film neural implants.

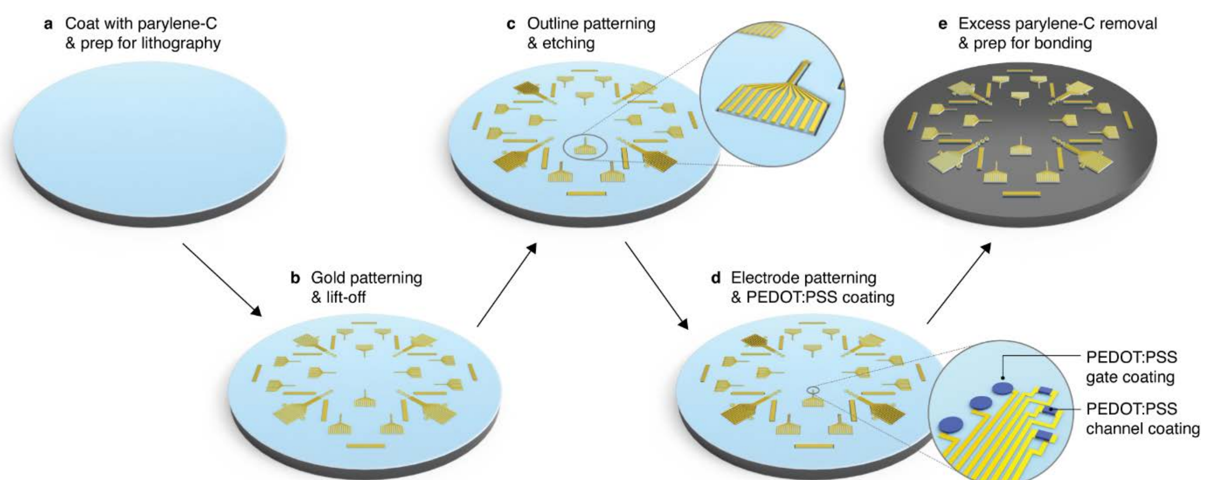

Fig. 2: Schematic of fabrication protocol
a, Thin-film bioelectronic devices are fabricated on silicon wafers coated with PaC. **b,** Au contacts, electrodes, and interconnects are defined with lithography and lift-off. **c,** An insulating layer of PaC is then deposited and a second photolithography step is used to define the outlines of each implant, followed by etching through to the wafer. **d**, After deposition of a sacrificial PaC layer, a final lithography step is used to define the areas for the PEDOT:PSS conducting polymer (electrodes, gates, and channels). PEDOT:PSS is spin-coated and the sacrificial PaC is removed. **e**, The devices are then ready to be removed from the wafer and prepared for bonding to flexible cables.

Here, we present a protocol for producing flexible, organic, thin-film bioelectronic devices. As noted above, the materials we described here are chosen from a wide range. This protocol provides an overview of the relevant materials, technologies and

experimental methods for the development and implantation of thin-film neural implants (Mask Design, Materials, and Procedures). Common issues faced during fabrication are discussed, and methods to overcome these challenges are presented (Troubleshooting). The electrical characteristics and the meaningful device parameters of the devices are highlighted and examined (Characterization). Finally, the protocol is summarized and potential applications are presented (Conclusion).

Expertise needed to implement the protocol:

This protocol is a tricky and time-consuming process with lots of pitfalls and caveats for those without requisite knowledge of fabrication for flexible devices. This detailed, in-depth protocol will comment on the main errors of failure and provide ways for mitigation, making this protocol accessible without any additional expertise needed to implement the protocol. It is important to note that this protocol requires access to a cleanroom facility.

Experimental design:

Optimal fabrication outcomes are contingent upon a well-designed mask (Fig. 3). The radial inhomogeneity inherent in the application of resist via traditional spin-coating methods, compounded by the occurrence of edge beads, can introduce pattern disparities in lithography and etching. To mitigate these effects, we advise the strategic distribution of devices radially on the wafer, ensuring a minimum clearance of 5 mm from the wafer's edge. Additionally, positioning critical elements such as electrodes and transistor channels towards the wafer's centre exploits the more uniform resist thickness in that region, enhancing accuracy and homogeneity. This approach enhances the accuracy and homogeneity of the active portions across different devices from within the same wafer. Our proposed protocol involves three lithographic steps, requiring the design of three masks to pattern (1) Au tracks (Fig. 3a), (2) the device outline (Fig.3b), and (3) the electrode / transistor openings (Fig.3c).

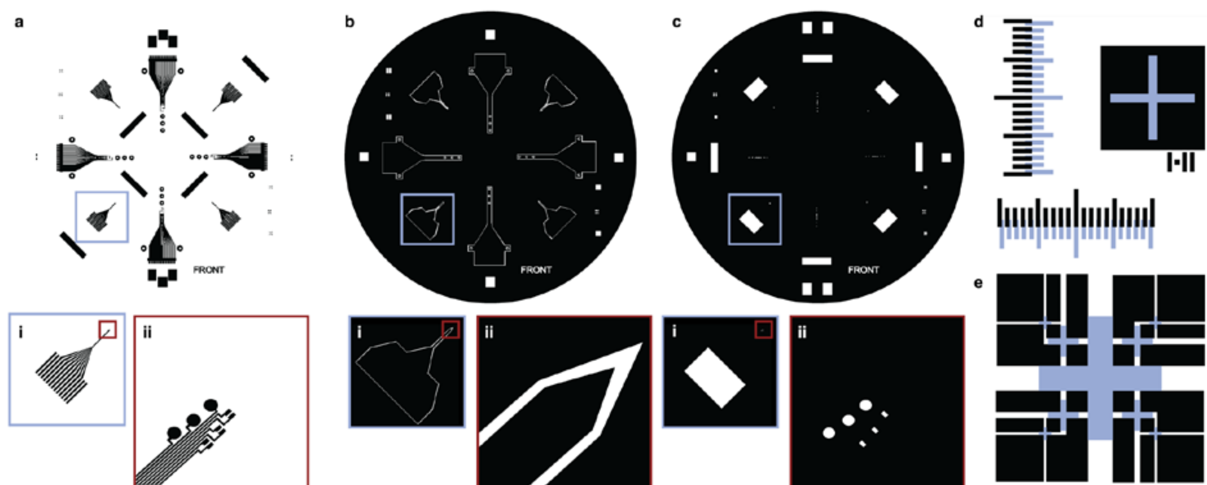

Fig. 3: Mask design and alignment marks
Mask designs used **a**,**i,ii** Au, **b,i,ii** outline, and **c,i,ii** electrode/channel patterning for the fabrication of the thin-film neural implants. Tone differences in the masks align with the corresponding positive and negative photoresists used in the different fabrication steps. Note that the electrode design[42] and the OECT design[43] are both based off previously published work. The CAD file for this design is included in the SI. **a**,**b**,**c**, Overall mask appearance. **i**, Inset (blue) showing electrode tip. **ii**, Inset (red) showing magnified electrode area. **d**, Vernier marks for mask alignment with devices containing sub-10 μm features, where Au patterning is shown in blue and subsequent mask pattern is shown in black. The cross has a line-width of 10 μm. **e**, Alignment marks for masks without high precision alignment constraints, where Au patterning is shown in blue and subsequent mask pattern is shown in black. The smallest cross (corners) has a line-width of 20 μm.

For most use cases, bioelectronic devices need not push the resolution limits of photolithographic fabrication methods. For example, a standard neural recording electrode for resolving single units should be approximately 20 μm in diameter. Feature sizes therefore typically afford leniency and are within the constraints of standard photolithography resolution limits.

For alignment of these sub-10 μm features, Vernier scales (Fig.3d) are needed for correct alignment in between different photolithographic layers, as they provide feedback of misalignment errors down to their micrometer scale and enable their compensation. However, for feature size higher than 10 μm, a set of crosses of different sizes are sufficient for alignment with sufficient precision to accommodate many patterns (Fig.3e). For increased precision, alignment markers must be placed near the outer rim of the wafer to minimize rotational misalignment errors. We recommend that 4 markers are placed on the 4 “corners” of the outer rim.

Materials
Reagents
CAUTION
Some of the chemicals mentioned in this protocol are hazardous and should, therefore, be handled with precaution, using appropriate PPE and following good laboratory practices. All the reagents should be disposed safely according to the local regulations.

- 4 inch silicon wafers (Microchemicals GmbH, cat. no. WSM4052525XB1314SNN1)
- AZnLOF 2035 (Microchemicals GmbH, cat. no.1A20350250) CAUTION Flammable liquid and vapour. Causes serious eye irritation. Always spin coat and bake inside a fume hood with proper ventilation.
- AZ 726MIF (Microchemicals GmbH, cat. no. 1000726). CAUTION Contains Tetramethylammonium hydroxide (TMAH). Causes severe skin and eye

damage. May cause damage to organs through prolonged and repeated exposure. Wear appropriate skin and face protection

- AZ 10XT 520cP (Microchemicals GmbH, cat. no.1A10xt0250) CAUTION Flammable liquid and vapour. Causes serious eye irritation. Always spin coat and bake inside a fume hood with proper ventilation.
- Parylene-C dimer (Specialty Coating Systems, cat. no. 980130-C-500GE)
- PEDOT:PSS (Heraeus Clevios, PH1000, cat. no. 81076212)
- 3-Glycidyloxypropyl)trimethoxysilane (Sigma Aldrich,, cat. no. 440167) CRITICAL. Moisture sensitive. Store in a dry environment, according to manufacturers specifications
- Ethylene glycol (Sigma-Alrich, cat. no. V000136)
- 4-Dodecylbenzenesulfonic acid (Sigma Aldrich, cat. no. 44198) CAUTION Causes severe skin burns and eye damage. Always use in a well ventilated area.
- Micro90 (Cole-Parmer Essentials, Fisher Scientific. cat. no. 11729989) CAUTION Contains Na, check if your cleanroom allows this.
- 0.45 µm polytetrafluoroethylene filter (VWR, cat. no. GILSANP1345)
- Flat flexible cables (Molex, cat. no. 15015-0233)
- Anisotropic conductive film (ACF) (3T Frontiers, cat. no 3T-TGP20500N-20x5.0x10M)
- Poly(ethylene glycol) (Sigma Aldrich, cat. no. 89510)
- Medical-grade poly(dimethyl siloxane) (World Precision Instruments, cat. no. KWIK-CAST-S)
- Dental Cement (parkell, C&B Metabond® Quick Adhesive Cement System)
- Isoflo® Isoflurane, 100 v/v% (Zoetis) CAUTION Isoflurane is an anaesthetic compound and should only be used in properly ventilated areas. Isoflurane is an anaesthetic inhalant and may be considered a controlled substance in some countries.
- Rimadyl, 50mg/mL (Zoetis) CAUTION Rimadyl is an analgesic pharmacological agent and may be considered a controlled substance in some countries.
- Metacam® Meloxicam, 1.5mg/mL (Boehringer Ingelheim Ltd., Animal Health) CAUTION Meloxicam is an analgesic pharmacological agent and may be considered a controlled substance in some countries.
- 50 µm Tungsten Microwire Shuttle (California Fine Wire Company)

Equipment

- MA/BA6 mask aligner (Karl Suss) using i-line with 120 mW/cm2.
- Oxygen plasma (Diener Electronic Femto)
- PVD-75 e-beam evaporator (LEV Kurt J Lesker)
- Parylene coater (PDS 2010 LABCOATER, Specialty Coating Systems)
- Reactive ion etcher (Oxford 80 Plasmalab plus, Oxford Instruments)
- Fineplacer pico (Finetech GmbH)

- Profilometer (Dektak XT)
- Isoflurane Vaporizer and Associated Induction/Recovery Equipment (Kent Scientific)
- Stereotaxic Frame (World Precision Instruments)
- Intan RHS Stim/Recording System (Intan Technologies)
- Intan RHS 32-Channel Stim/Recording Headstage (Intan Technologies)

Procedure

Parylene-C Coating

1. Number the wafer for traceability across the process. This can be done using a solvent resistance marker.
2. Deposit 2 µm of PaC onto the silicon wafer using 4 g of dimer (furnace 690˚C, chamber 135˚C, 20-26 mTorr, 690˚C, vaporizer 175˚C set point). Confirm thickness on a dummy sample using a spectrometer or profilometer.

Lithography for Au deposition

3. The first photolithography step defines the metal electrodes, contacts, and interconnects (Fig.3a). Spin-coat the negative photoresist, AZ nLOF 2035, onto the substrates (1500 rpm, 1000 rpm/s for 30 s for 3.5 µm). Soft bake for 120 s at 115˚C. Cool down for 120 s. Align with the mask aligner and UV expose 150 mJ/cm^2 with hard contact. Post exposure bake for 60 s at 115˚C. Develop for 120 s in AZ 726 MIF, agitate (slowly shake the beaker anticlockwise every 30 seconds or use an automatic shaking plate set to ~40 RPMs) solution during development. Rinse with DI water, and dry with N_2 gas
4. Examine under the microscope for undeveloped resist in the developed tracks. The tracks should be clean and without texture.

Comment: AZ 400K has better wettability than AZ 726 MIF. For critically small feature size, dilute AZ 400K in deionized water at a 1:4 concentration. Use at least 50 mL. Note that developer is ‘spent’ during development, meaning fresh developer will develop faster than developer that has been used at least once.

Au Evaporation

5. Activate for adhesion immediately before metal deposition with 60 s of oxygen plasma (25 W, 0.8 mbar, Diener Electronic Femto).
6. Deposit 10 nm of Ti (0.3 Å/s, approx. deposition info: power = 430 W, current = 21.4 mA) and 100 nm of Au (0.6 Å/s, approx. deposition info: Power = 980 W, current = 49.5 mA) using an e-beam evaporator (Kurt J Lesker PVD-75) (Fig.4a).

Lift-off

7. Place wafers in acetone for 15 minutes to lift-off (Fig.4b). Gentle cleaning with a swab can be used to assist lift-off, but do not sonicate as this will damage the devices. If it is a hard lift-off (longer than 2 hours) change to Technistrip®

NI555 (Technic Inc.). Long acetone lift-offs cause pinholes in the PaC film. See Table 1 for troubleshooting.

8. Rinse the wafer with acetone while carefully extracting it from the dish. This step serves to prevent any potential adherence of Au particles onto the wafer surface.
9. Rinse with IPA.
10. Inspect the wafer under a microscope after rinsing and covering it with IPA. Drying the wafer without inspection may result in difficulty removing undeveloped parts. If any undeveloped small bits are observed, they can be gently swabbed off under the microscope.
11. Rinse with DI water and dry with N_2 gas (Fig.4c).

Fig. 4: Detail of lift-off process

a, Pristine Au layer after deposition of Au in the LEV. **b**, Partial lift-off of some features, where layers of Au can be seen detaching from the surface. **c**, Complete lift-off of the wafer with no remaining of Au in between features. Scale bar approximately 10 mm.

Parylene-C coating (insulation layer)

12. Deposit the PaC insulation layer, following the same procedure as Step 2.

Lithography for outline layer

13. The second lithography step defines the outlines of individual devices (Fig.3b). Spin-coat a positive photoresist, AZ 10XT, at 3000 rpm, 8000 rpm/s for 30 s for 5 µm. Soft bake for 2 minutes at 115˚C. Rehydrate in a 50+% humidity chamber for 30 minutes. Align and expose in equal 2 doses with 10 s between, totalling 600 mJ/cm^2. Check light intensity at 365 nm to adjust sector exposure time. Exposure time can be calculated as: exposure time = 600 mJ/(15.6 mW*0.78) ~ 49.3 s. Split exposure into 3 parts: e.g., 16 x 3 times. See Table 1 for Troubleshooting.
14. Develop in AZ 726MIF for 10 minutes, agitate from time to time, rinse with DI water, and dry with N_2 gas.

RIE etching

15. Etch through the 4 µm PaC using a reactive ion etcher (Oxford 80 Plasmalab plus). We use 8.0 sccm CF_4, 2.0 sccm SF_6, and 50 sccm O_2 , forward bias

180 W. This gives a 200 nm/min etch rate requiring 25 minutes to etch through 4 µm PaC. This can also be achieved using a longer, pure O_2 etch. Rinse with acetone to remove any remaining photoresist and dry with N_2 gas.

16. Examine the etched areas under a microscope. Presence of residual photoresist and PaC is typically indicated by the appearance of rainbow or burnt-like shades on the etched surface (Fig. 5a). If PaC residue is detected, repeat step 15 to ensure complete etching (Fig.5b).
17. Rinse with acetone and IPA.

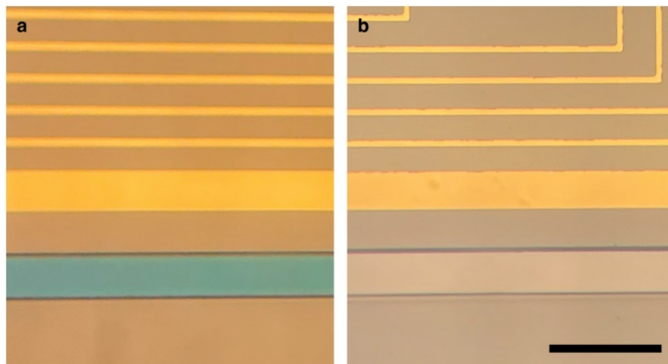

Fig. 5: Detail of RIE etching

a, Outline of thin-film neural implant where the outline is not completely etched and hence a thin layer of PaC shaded blue is visible. **b**, Fully etched outline of a thin-film neural implant. Scale bar represents 100 µm.

<u>Parylene-C coating for peel-off layer:</u>

18. Prepare a 2% micro-90 solution in DI water and spin-coat at 1000 rpm for 30s. Dry at ambient temperature in the hood for 2 minutes and repeat one more time for each wafer. The addition of this intermediate layer enables PaC peel-off.
19. Deposit the third PaC layer, again with the same procedure as Step 2.

<u>Lithography for PEDOT:PSS coating</u>

20. The 3rd and final lithography step (Fig.3c) is used to expose the electrodes, contact pads, and / or OECT channels. Use a positive photoresist, AZ 10XT and follow the same procedure as Step 13 (Fig.6a). See Table 1 for troubleshooting.
21. Pop any bubbles that form with a needle. Bubbles can burst during the RIE process potentially causing damage to the wafer. The air will move under the PaC layer to find the escape. While it's advisable to eliminate as many bubbles as possible, small ones left may not significantly impact the process. If the bubbles are present on the contact pads or electrodes, they should not be pierced directly but instead the PaC layer adjacent to them should be pierced to give any vapor a route to escape.

22. Etch through the top 2 PaC layers using the same procedure as Step 15, with caution to not over-etch the substrate. If there is PaC left, there are usually visible debris on the Au surface (Fig.6b,c). See Table 1 for troubleshooting.

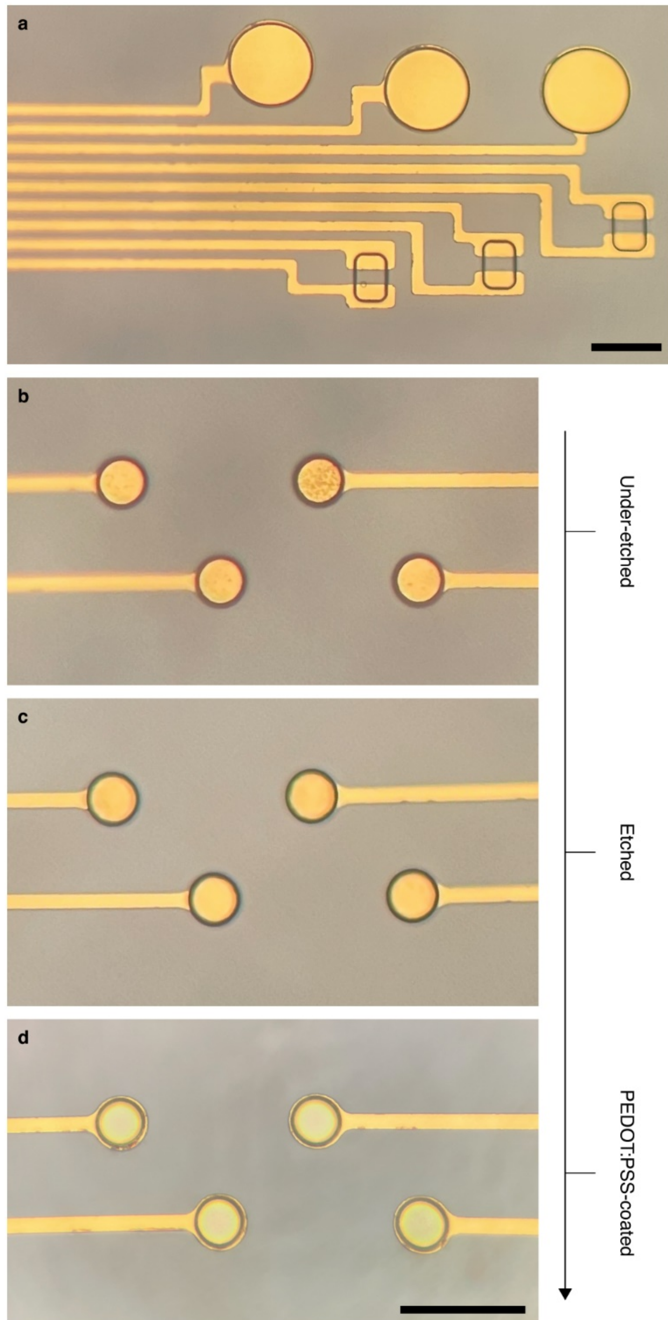

Fig. 6: Detail of electrode RIE etching and spin-coating
a, Developed AZ 10XT photoresist mask for etching the openings in the gates and channels of the OECTs. **b**, Under-etched electrodes in which a layer of rough PaC is visible near the openings. **c**, Fully etched electrodes where the Au is visibly clear and homogeneous in all the openings. **d**, PEDOT:PSS-coated electrodes in which the shade of green is indicative of the polymer coating of the Au contacts. Scale bars represent 50 µm.

PEDOT:PSS spin-coating (timing 2 h)

23. Mix Clevios^{TM} PH1000 PEDOT:PSS with 5% (v/v) ethylene glycol (EG, enhances conductivity) and 0.25% (v/v) 4-Dodecylbenzenesulfonic acid (DBSA, improves film homogeneity). Sonicate for 15 minutes. Prepare approximately 10 mL for each wafer.
24. Add 1% (v/v) 3-Glycidyloxypropyl)trimethoxysilane (GOPS, crosslinker) to the PEDOT:PSS blend, and sonicate for 1 minute.
25. Filter using 0.45 μm polytetrafluoroethylene filter, discarding the first few drops.
26. Activate substrates with oxygen plasma, using 100% power with 30% O_2 for 60 s.
27. Spin-coat the PEDOT:PSS blend onto substrates at 3000 rpm for 30 s.
28. Gently swab the contact area with a large swab dampened in DI water to remove any PEDOT:PSS residue and prevent potential short circuits.
29. Soft bake for 1 minute at 110˚C.
30. Depending on the desired thickness, 1 or more additional PEDOT:PSS layers can be spin-coated, each followed by a 1 minute soft bake (Fig.6d). It is important to work quickly during this process, as the crosslinking reaction of begins upon the addition of GOPS. Each layer deposited is ~ 90 nm thick, we recommend depositing three layers of PEDOT:PSS totalling 270 nm.

Peel-off

31. Immediately following the PEDOT:PSS soft bake, lightly scrape the edge of the wafer with a razor blade to loosen the top PaC layer (Fig.7a).
32. Gently place a piece of tape on the edge of the wafer. Slowly and evenly use the tape to peel off the sacrificial PaC layer. Tweezers can also be used for peeling the sacrificial layer of PaC (Fig.7b). See Table 1 for troubleshooting.
33. Hard bake to crosslink PEDOT:PSS for 1 hour on a 130˚C hotplate.
34. Place in DI water overnight to remove excess acid and low molecular weight solvents from the PEDOT:PSS. Note that PEDOT:PSS coatings will be visible under the microscope and can vary slightly in their coloring based on the size of the coated feature (Fig.6d).

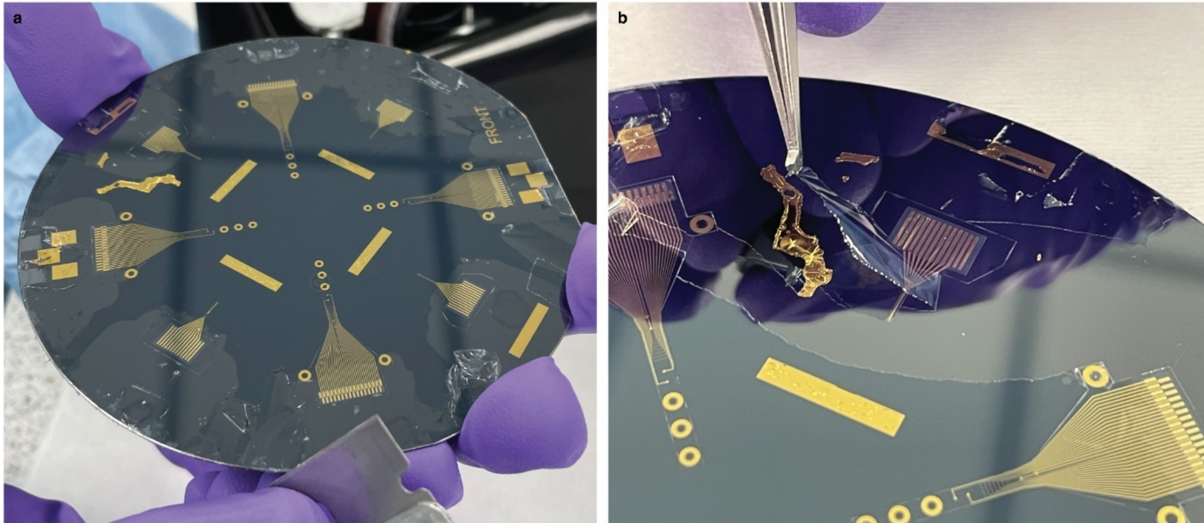

Fig. 7: Peel-off of sacrificial layer of PaC
a, Scraping the edge of the wafer with a razor blade breaks the PaC continuity between top and bottom of the wafer. **b**, Tweezers can be used to peel off the sacrificial layer of PaC that comes off easily from the insulation layer thanks to the release soap. Scale bar represents 100 μm.

<u>Bonding</u>

35. Peel off individual devices from the wafer. Use water and a brush to release from the silicon and transfer to glass slides (Fig.8, Video S1). Make sure devices are flat, with no wrinkles. This can be achieved by placing the devices onto a hotplate at 80˚C and using water and a brush to remove the wrinkles. See Table 1 for troubleshooting.

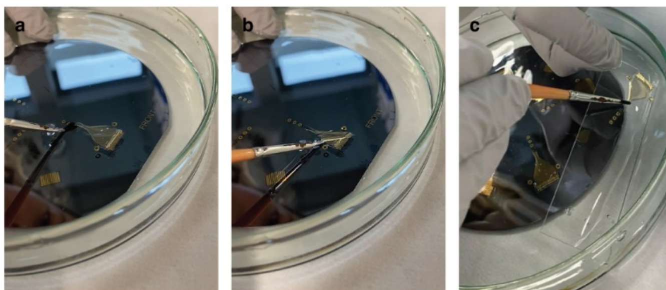

Fig. 8: Device removal from wafer
a, Submerging the wafer in DI water helps detachment of the device from the wafer. **b**, With the aid of a soft brush, peel the device from the wafer. **c**, Lay the device flat on a glass slide. If wrinkles are formed, a droplet of water and careful brushing can make it flat.

36. For best bonding results, place the devices onto a hotplate at 80˚C for an hour before bonding to remove excess water from below the device.
37. Prepare ACF tape, cutting only enough needed for the devices needing bonding.

38. Place substrate on heating plate (set to 55˚C) of the bonder (Fineplacer pico (Finetech GmbH) or similar) and switch vacuum on (Fig.9a).
39. Align bonding area of substrate with head.
40. Focus head and focus substrate.
41. Remove anisotropically conductive film (ACF) from the refrigerator and allow to reach room temperature.
42. Place ACF tape on the pad area (Fig.9b) and align with the head (set to 80˚C), cover substrate and ACF with a protective black silicone sheet (Fig.9c).
43. Using a 200 N load, approach, and contact substrate for 4 s.
44. Remove ACF liner and align substrate with flex cable (Fig.9d,e).
45. Focus head and flex cable.
46. Apply 200 N for 2 s, switch off vacuum and lift.
47. Change force to 500 N, contact head to substrate and switch off vacuum.
48. Start bonding process: heating plate at 70˚C, head temperature ramping from 55˚C to 200˚C at 20˚C/s, plateau for 25 s then ramp back down, leave sample to finish cooling (Fig.9f). See Table 1 for troubleshooting.

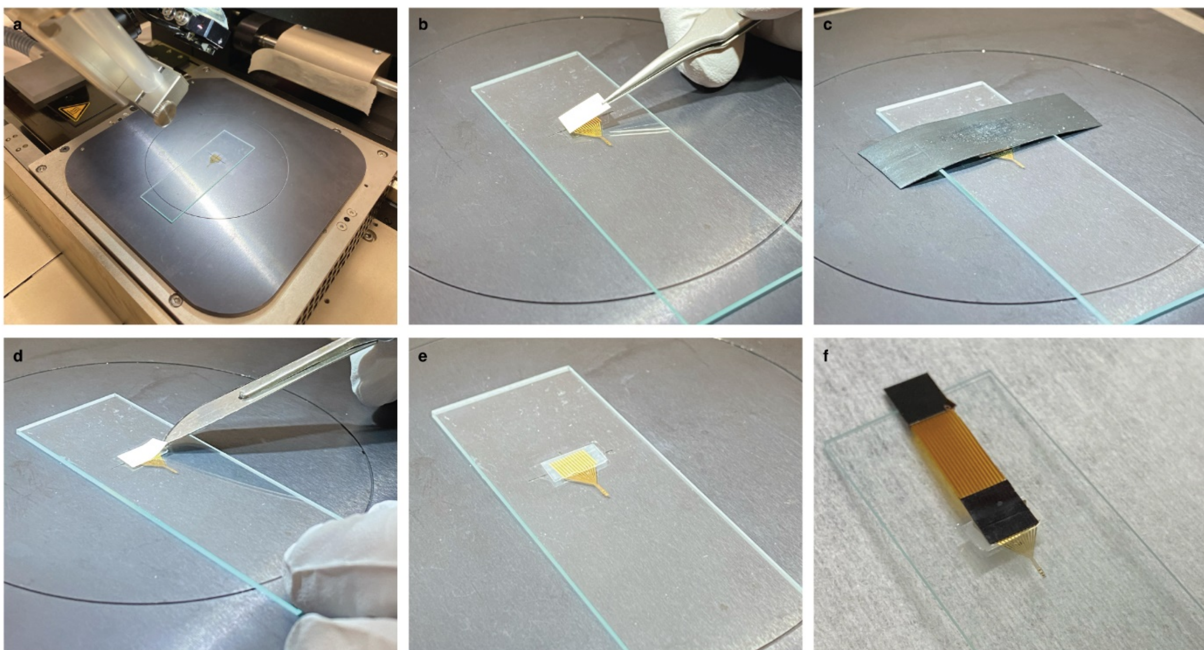

Fig. 9: ACF bonding of the device with a flexible cable
a, Place the device on the hot surface of the bonder for pre-bonding and alignment. **b**, ACF tape, sized to the contact pad for bonding, is placed on the device for electrical contact with the cable. **c**, A protective piece of silicon sheet is placed on top of the tape for pre-bonding step. **d**, After pre-bonding, the liner is removed from the ACF tape. If detachment is difficult, a scalpel can be used to assist in backing removal. **e**, When the tape is exposed, align the contact pads of the device and the cable. **f**, Apply pressure and heat to bond the cable onto the device, finishing the connection.

<u>Characterisation</u>

49. To check the electrodes, measure the impedance spectrum using electrochemical impedance spectroscopy (EIS).We apply a 10 mV sinusoidal voltage over a frequency range of 0.1 to 100,000 Hz and monitor the resultant sinusoidal current of the system. The input signal can be mapped to the output signal using a transfer function that allows us to extract the instantaneous impedance at different frequencies. The EIS measurements were conducted using an Autolab PGSTAT128N, where the array's electrodes served as the working electrodes, and a large 1 cm×1 cm platinum electrode functioned as the counter electrode.
50. To check the OECTs and to measure transfer and output characteristics. A series of preconditioning scans helps to remove excess low molecular weight solvents, improving stability [44]. We use a series of 11 output cycles with V_G ranging from −0.5 to 0.5 V (0.1 V steps) and V_D ranging from −0.6 to 0.05 V (bidirectional). Output curves are followed by a series of 5 transfer cycles with V_D stepping from −0.1 to −0.5 V and V_G ranging from −0.5 to 0.5.

All characterisation measurements should take place in 0.01 M PBS.

<u>Pre-operative Preparation (Mouse or Rat)</u>

51. Move animal into induction chamber on heating pad.
52. Increase isoflurane content to 5% partial pressure until animal is anaesthetised.
53. Decrease isoflurane content to 2.5% partial pressure and place animal onto facemask in preoperative area on heating pad to prepare surgical site.
54. Collect pre-operative weight for post-operative monitoring as well as determining dosages for fluid replacement and analgesic management.
55. Inject saline subcutaneously for fluid maintenance during surgical procedure.
56. Inject pre-operative analgesic (Rimadyl) subcutaneously for pain management.
57. Clip claws to reduce likelihood of animal interacting with resultant sutures during recovery post-operatively.
58. Shave the surgical site, ensuring that the surrounding area is free from fur.
59. Clean the surgical site, beginning at the center of region and working outwards to reduce possibility of contamination during surgery.
60. Move animal to surgical station, maintaining isoflurane at 2.5% partial pressure.
61. Use rectal thermometer with heating pad to maintain animal’s body temperature throughout surgical procedure.
62. Check paw withdrawal reflex prior to initiating surgery to ensure appropriate anaesthetic depth before making initial incision.
63. Thin-film neural interfaces are highly compatible with long-term tissue response but also must be placed very carefully. Devices should only be handled when wet and care should be taken to prevent application of

unnecessary tension to device during surgical procedure. All tensile movements should be accommodated for through excessed parylene, to allow for movement through translations and un-buckling of device rather than through simple tension, as parylene is a relatively stiff material and can tear. Within these bounds, operative surgical procedures can vary substantially (Fig.10) depending on location for device placement. Note that in all cases, all equipment used must sterilized for use in aseptic surgical procedures. Further, a majority of surgeries involving the placement of thin-film devices are considered microsurgeries, to be performed under a stereo microscope, to aid in placement. Extensive practice for microsurgical work (cadaveric) is recommended prior to performing surgery. Numerous countries, including the UK where this protocol was performed, also require various licensing mechanisms to perform this work. Thin-film devices have been used in various other locations around the body, such as the gut[42] etc. A thorough review of literature should be conducted prior to surgical development in all cases to ensure best practice and reduce unnecessary suffering for animals in these studies, inclusive of reduction in number of animals utilized. The following sections outline four potential methods for device placement into different tissues, as has been performed in prior studies [22,45,46].

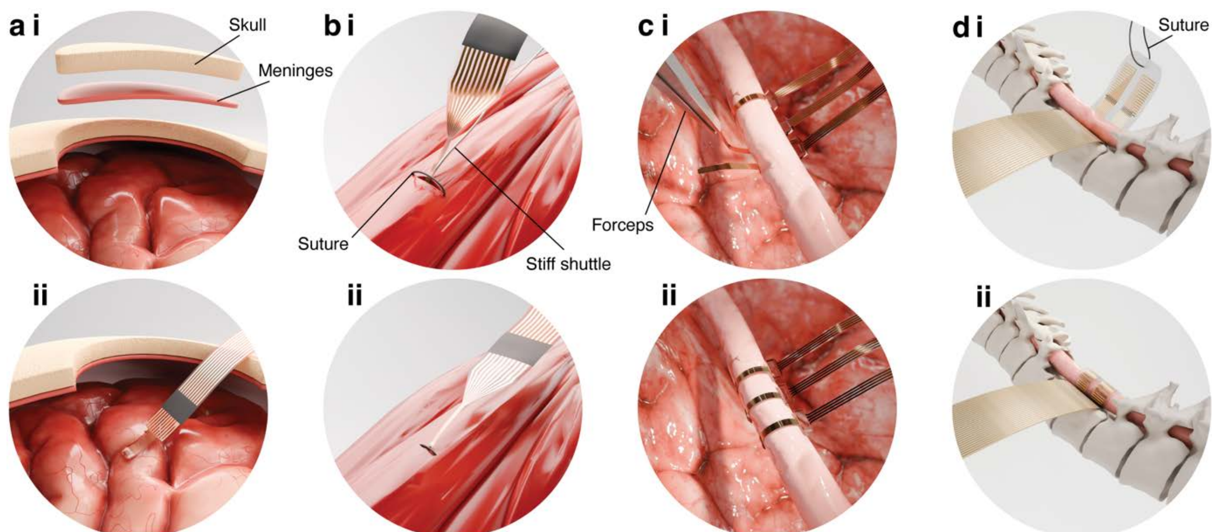

Fig. 10 Schematic of implant placement.
a, Schematic showing placement of a microelectrode array for electrocorticography. **i**, Initially a craniotomy is performed to remove a portion of the skull above the desired location for the implant. Typically the dura is also removed to allow direct electrical access to the brain tissue. **ii**, For electrocortigraphy, the device is placed directly onto the cortex. **b**, Schematic showing placement of an intramuscular implant. **i**, Initially, an incision is made into the musculature, into which the implant is placed. Placement is typically performed using a shuttle to accommodate the flexibility of thin-film neural implants. The neck of the implant can then be sutured to prevent back-sliding of the device out of the incision. **ii**, The device and suture are left in place for the desired application. **c**, Schematic showing placement of a nerve

cuff, in this case containing three distinct cuffs to illustrate closing of the cuff. **i**, After isolation of the nerve the cuff can be wrapped around the nerve using forceps before closure, typically using an in-built design feature, a suture, or a medical-grade adhesive. **ii**, After placement cuffs should remain in close contact with the nerve to provide an appropriate electrical interface with the tissue. **d**, Schematic for placement of a spinal cord implant. **i**, After isolation of the desired section of spinal cord, the implant should be slipped under the spinal cord using a suture to pull the implant through and around the tissue. **ii**, the leading edge of the device should then be tied back onto the trailing edge using a similar mechanism to the nerve cuff to precent implant movement post-placement.

<u>Electrocorticography Array Placement (Fig.10a)</u>

a. Place animal into stereotaxic frame, confining head movement using ear bars.
b. Check head stability from ear bar placement prior to making incision.
c. Make incision in the center of the animal's scalp, pulling back tissue to reveal the skull.
d. Remove excess tissue to ensure boney surface for following steps.
e. Score skull surface for screw placement above the cerebellum at the base of the animal's skull, approximately 3mm caudal to the animal's lambda. This location provides some space above the brain's surface, reducing likelihood of damage to the brain upon screw placement. However, small (<1mm in length) screws should be used.
f. Drive screw through the skull to contact cerebrospinal fluid to act as ground for recording.
g. Wrap steel wire around ground screw to provide access to ground for subsequent recording.
h. Determine implant location using stereotaxic coordinates and score area around this region using surgical drill.
i. Using surgical drill, perform craniectomy, taking care to prevent pressure or damage to the underlying tissue.
j. Remove any excess asperities from around the craniectomy window to reduce possibility of damage post-operatively.
k. For some recording cases or intra-cortical placements, carefully remove dura prior to device placement. Dura removal can be effectively performed using a small-gauge needle to 'hook' the dura. Craniectomy and dura should be removed as 'late' in the surgery as possible to prevent unnecessary swelling in conjunction with changes in intracranial pressure.
l. Position device on top of the cortex for electrocorticography or bind device to stiff shuttle (typically tungsten microwire or small needle, 30G or smaller) by dipping device into solution containing low molecular weight poly(ethylene glycol) at 10w/v% [45] or similar and allow device to dry and adhere to shuttle. Using this method for intra-cortical placement, lower shuttle into the cortex to the desired depth using the stereotaxic frame and allow ~5min for dissolution

of poly(ethylene glycol) binder. Carefully remove shuttle, leaving thin-film device within the cortex.

m. Inject medical-grade poly(dimethyl siloxane) into the craniectomy window to seal the region around the implant.
n. Apply dental cement above the poly(dimethyl siloxane) to cement implant to the skull.
o. Place headcap or similar structure to allow either tethered access to the implant or placement of a wireless coupling mechanism. Headcap design can vary substantially to accommodate implant and connector design. Headcaps are often custom-made for this purpose.
p. Enclose headcap to prevent tampering by animal.
q. Suture skin around headcap, ensuring tight closure around the percutaneous juncture.

Intramuscular Implant Placement (Fig.10b)

a. Make incision above desired muscle group to prepare for access to peritoneal cavity.
b. Perform Step b. through Step e. from Nerve Cuff Placement for percutaneous port placement.
c. Return to initial incision site and make small incision using fine surgical scissors into musculature.
d. Adhere device to shuttle, as described in Step l. from Electrocorticography Array Placement.
e. Position device within intramuscular incision, and remove shuttle after binder dissolution, as above [45].
f. Suture a loop around the base of the device to prevent movement of the device out of the desired location. Consider design of suture loop on the front of the device to run a suture into the incision, guiding the implant along this path, then suturing this front loop to prevent device from sliding backwards.
g. Perform Step i. and Step j. from Nerve Cuff Placement

Nerve Cuff Placement (Fig.10c)

a. Make incision in the vicinity of nerve of interest.
b. Make secondary incision for placement of percutaneous access port. Numerous methods exist for port placement. For recordings in the peripheral nervous system, port placement above the shoulder blades in recommended to prevent animals from tampering with port post-operatively. Port design can vary substantially to accommodate implant and connector design. Ports are often custom-made for this purpose.
c. Using blunt dissection, create tunnel from initial incision to port incision.
d. Run subcutaneous wires along this incision pathway to provide location for placement of plugs for tethered recordings or wireless method.

e. Place percutaneous port containing group wiring and suture surrounding tissue using sub-cuticular technique to prevent any movement of port post-operatively.
f. Return to initial incision site and carefully dissect away tissue, ideally maintaining location to between muscle groups to prevent muscular damage and recovery complications.
g. Locate and isolate nerve of interest and wrap nerve cuff around nerve.
h. Set device circumference around nerve either using in-built (designed) locking mechanism and/or small drop of medical grade poly(dimethyl siloxane).
i. Depending on nerve location and degree of dissection necessary to reach nerve, consider placement of layered sutures to limit internal damage and improve healing times during recovery. Internal sutures can be placed using simple interrupted or simple continuous techniques, depending on the size and severity of the internal incisions.
j. Suture outer incision site closed using sub-cuticular technique to prevent animals from tampering with device.

Spinal Array Placement (Fig.10d)

a. Make incision at desired level on the spine for device placement.
b. Perform Step b. through Step e. from Nerve Cuff Placement for percutaneous port placement.
c. Return to initial incision site and perform laminectomy to expose the spinal cord.
d. Clip the pedicles using a rongeur and perform blunt dissection to access the epidural space.
e. Tie suture to leading edge of the implant and guide the implant into place on top of or around the spinal cord, tying off the suture to prevent sliding [46].
f. Place medical grade silicon above the device to secure it in place.
g. Perform Step i. and Step j. from Nerve Cuff Placement.

Post-operative Recovery

2. Remove animal from face mask and record post-operative weight (to account for placement of additional components – percutaneous port, implant, wiring, etc.).
3. Move animal into heated recovery chamber and monitor during recovery from anaesthesia.
4. Provide analgesia (Meloxicam, usually delivered orally) to animals on Day 1 and Day 2 post-operation, and monitor animal weight, ensuring that weight is maintained, indicated healthy recovery.

Recording / Stimulation & Post-processing (in brief)

5. Numerous instruments can be used for recording neural activity from these types of devices. In all cases, the bonded connector (Steps 35 - 50) must be

interfaced back to the desired equipment. This is typically accomplished using a custom printed circuity board with surface-mount plugs to convert the flat array of microfabricated channels to a 3D plug for integrated circuit interfacing. The exact mechanisms for interfacing depend entirely on the backend equipment used for accessing the microfabricated device. As an example, a commonly used instrument for interfacing with electrode-based devices is the Intan RHS Stim/Recording System. Intan produces headstages that can be integrated with devices constructed through the above protocol through the construction of printed circuit boards containing an Omnetics connector to plug into the Intan headstage. In the case of a Molex flexible flat cable, a zero-insertion force connector can be surface-mounted to a custom printed circuit board to run channels from an electrode-based device to the accompanying Omnetics plug to connect to the headstage. Using this setup, plug the device into the associated headstage and connect the ground wire to the headstage for *in vivo* recording or stimulation.

6. Post-processing of recorded data is beyond the scope of this protocol, but various forms of signal analysis are typical, including application of various filters, spike identification and sorting mechanisms, and other more complex algorithmic approaches. Several in-depth books have been published on these topics, and we also recommend following current research in the field for the most up-to-date methodologies [47–51].

Timing

Timing is standardized for processing a batch of 3 wafers. Equipment variations may permit a different number of wafers, necessitating adjustments to the protocol timing. Our current setup accommodates processing 3 wafers simultaneously. Break points in the fabrication process are recommended if continuous flow is not feasible. During these break points and at the end of the fabrication process, the wafers/devices should be stored at room temperature with low humidity conditions.

Steps 1 - 2: 3 to 4 hours

Break point – stable for up to 1 month

Steps 3 - 4: 1 to 3 hours

Steps 5 - 6: 2 to 4 hours

Steps 7 - 11: 2 to 6 hours

Step 12: 3 to 4 hours

Break point – stable for up to 1 month

Steps 13 - 14: 2 to 4 hours

Steps 15 - 17: 2 to 3 hours

Break point – stable for up to 1 month

Steps 18 - 19: 3 to 4 hours

Steps 20 - 22: 3 to 4 hours

Steps 23 - 30: 2 to 3 hours

Steps 31 - 34: 1 to 3 hours

Break point – stable for up to 1 month

Steps 35 - 48: 1 to 3 hours

Steps 49 - 50: 1 to 3 hours

Total Timing for Fabrication: 26 – 48 hours

Steps 51 - 62: 10 minutes

Step 63: 10 minutes to 5 hours

Steps 64 - 65: 10 minutes to 1 hour (dependent on length-of-surgery / time under anaesthesia)

Step 66: not applicable

Step 67 - 68: not applicable

Total Timing for Surgery: 30 minutes to 10 hours

Troubleshooting

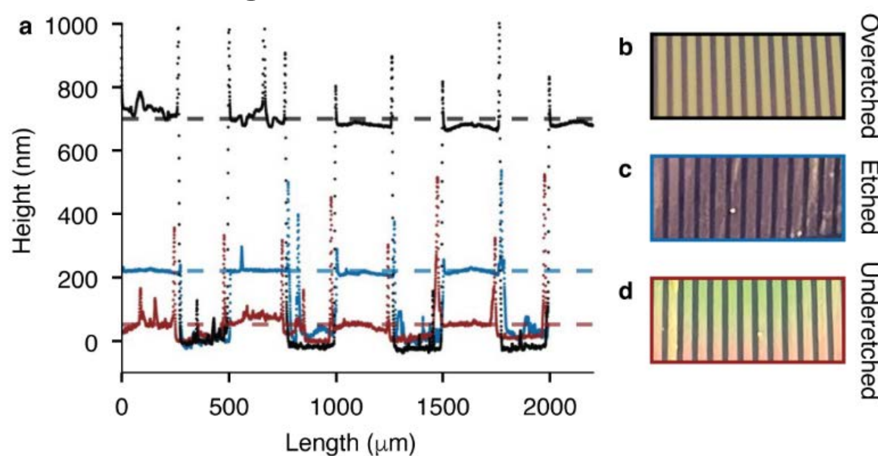

Fig. 11: Examples of profilometer data from under-etched, fully-etched, and over-etched insulation. a, Height profile showing images **b**, over-etched **c**, fully-etched, and **d**, under-etched contact pads. Similar results would be expected on the gold electrodes during insulation etching.

During the fabrication process, several problems can occur. The first of which is determining whether your device is correctly developed. This can be ascertained by optical microscopy and visualization. If you under-develop your sample, the areas where you need to remove further photoresist will have a rainbow appearance (Fig. 5). The pads and electrodes will appear cloudy, indicative of photoresist still present. Overdevelopment will result in removal of your smallest features up to all of your features from the wafer.

Development is likely to affect your lift-off process (Step 7). If you lift-off and find that the Au comes off the entire wafer it is likely that you have under-developed. If you lift-

off and find that the Au does not to come off, it is likely that you have over-developed and removed the majority of the photoresist. If you are struggling to perform Au lift-off for the devices, we recommend placing the beaker containing the devices and acetone onto an orbital shaker at 50 rpm in a horizontal position. This will encourage the lift-off process.

A potential issue with this protocol step is the lithographic patterning of the openings (Steps 13 and 20). The soap layer produces nitrogen gas when exposed to UV light during the patterning process. To mitigate the production of these gases, we recommend exposing in multiple doses, up to 5 with a 10 s gap in between. Some small bubbles may still be present, however these will not cause an issue during fabrication. If large bubbles persist (> 50 µm), we recommend lancing them with a small needle before etching to prevent them from expanding under vacuum during the etching process and damaging your devices.

A good protocol to ensure correct etching is measuring the PaC thickness after every deposition. For each layer of your deposition chamber, place a dummy sample (made of the same material as your substrate) adjacent to your wafer. Then, check the thickness using a profilometer post-deposition. To ensure consistent etching, calibrate your RIE, i.e. run a dummy sample prior to your samples to calculate the etching rate. Finally, to check for under or over-etching, take a height profile across the contact pads (Fig.11).

Bonding issues may arise due to poor maintenance of the ACF tape. The ACF tape should be stored at 4˚C in a stand-alone desiccator to prevent moisture damage. The tape should be handled delicately and cut with a rounded scalpel and handled with blunt tweezers to ensure minimal damage.

This fabrication process can consistently produce devices with feature sizes down to the scale of single microns. When using manual mask aligners, misalignment can cause issues in the outcome of the device, but these problems can be overcome with increased training and the use of Vernier or other high resolution alignment marks (Fig. 3d).

Table 1 Troubleshooting

Step	**Problem**	**Possible Reason**	**Solution**
7	Too much Au lift-off	Under-development	Longer photoresist development
7	Au doesn’t lift-off	Over-development	Shorter photoresist development and/or shake in acetone
13 and 20	Bubbles below PaC	Nitrogen gas induced by UV	Segment UV exposure during patterning and/or

			lance large bubbles with needle
22 and 32	PEDOT:PSS areas not exposed	Under-etching	Monitor PaC thickness with profilometry and etch cautiously
35	Devices too thin and rip during peel-off from wafer	Over-etching	Monitor PaC thickness with profilometry and etch longer if needed
48	Poor bonding adhesion	Damaged ACF tape	Store in dessicator at 4˚C and handle delicately
13 and 20	Misaligned features	Manual mask alignment	Use Vernier or other high resolution alignment markers

Anticipated Results

Characterisation is a necessary step for electronics microfabrication. Detailed methods and discussion regarding this subject can be found in numerous reviews on the subject [52–55]. For electrode-based devices, impedance is commonly used as a figure of merit (Fig. 12) [52]. Numerous electrophysiological recording setups will provide a single frequency measurement at 1 kHz, as 1 ms is the generally accepted length of an action potential. Of note, these devices can be used to record various signals at various frequencies, meaning that the appropriate frequency-dependent impedance value should be considered. As such, we recommend EIS as a way to fully characterize the outcome for the devices in question, with consideration of the impedance and phase angle measurements across a frequency range.

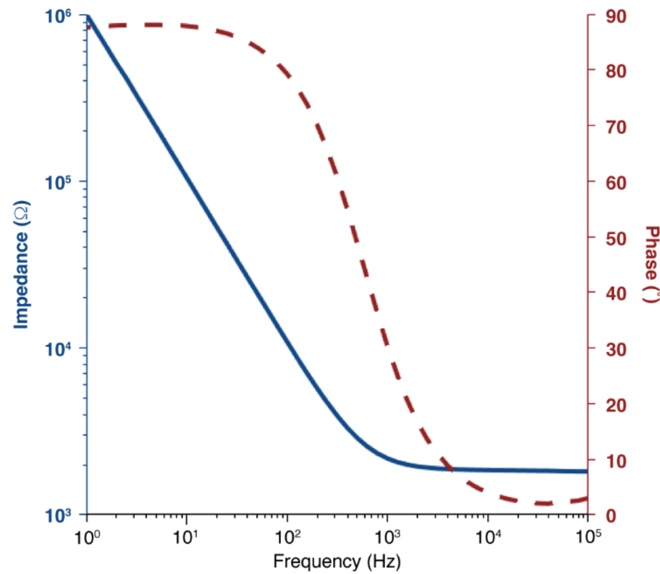

Fig.12: Representative electrode impedance
Representative bode plot, showing phase and impedance of implantable, thin-film device with PEDOT:PSS electrodes with a diameter of 200 μm.

For the outcome of the OECT devices, g_m on the value of ~1.2 mS can be expected for OECTs operated with Ag/AgCl gate with V_G = 0V and V_D = -0.5V (Fig. 13). Note that to maximize transconductance, as achieved when using an external Ag/AgCl gate, the planar PEDOT:PSS should be sufficiently larger than the channel. However, it should be noted that the gate and channel capacitances can be deliberately matched when a voltage drop at the gate is desired, for example to drive an electrochemical reaction [56]. Representative transfer and output measurements are shown with V_D stepping from −0.1 to −0.5 V and V_G ranging from −0.5 to 0.5 V, and measured with a Keysight B1500A semiconductor device analyzer. For further details on standard OECT characterization, see the guide published by Ohayon, et al.[57]. Note the relevance of channel dimensions for these measurements as well. High transconductance OECTs employ short channel lengths, which require precise alignment. Guidance for predicting transconductance upon changed parameters are discussed in the following reviews [58–60]. As an example from previously reported literature, specifically for in vivo applications where low power is desired, device geometry optimized for zero gate bias could be considered in the mask design. From this example, channel dimensions of W = 10 μm, L = 5 μm, and d ~ 140 nm were used, which yielded $g_{m,max}$≈2 mS at V_g = 0 V [61].

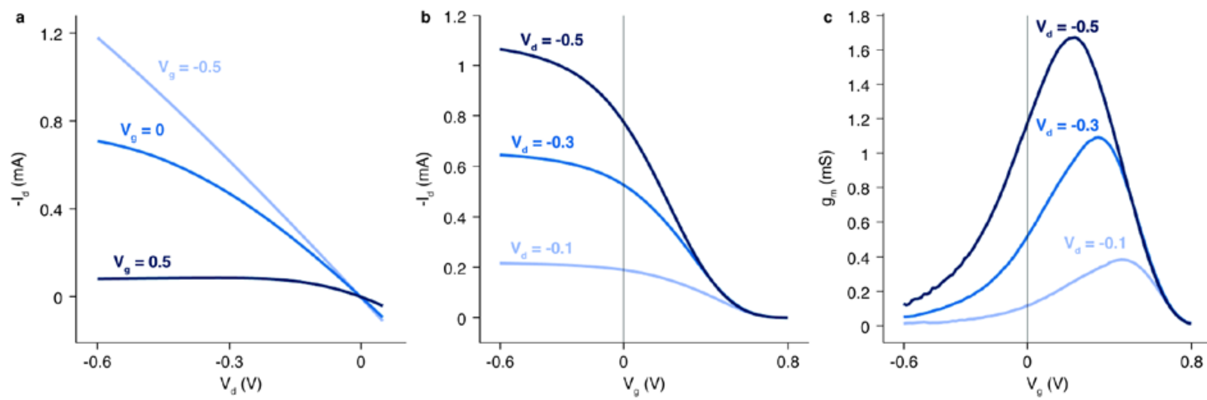

Fig.13: Representative OECT characteristics

Representative **a**, transfer **b,** output and **c**, transconductance of implantable, thin-film PEDOT:PSS OECTs operated with an Ag/AgCl gate and channel dimensions 10 x 20 μm.

Finally, we show the variation in impedance as a function of electrode size through the production of numerous devices per this protocol (Fig. 14). It is important to note that feedline length, width, and PEDOT:PSS thickness can also influence electrode impedance [62]. We also demonstrate protocol consistency, plotting impedance at 1 kHz from electrodes from these devices across six different wafers from two independent fabrication runs (Fig. 14).

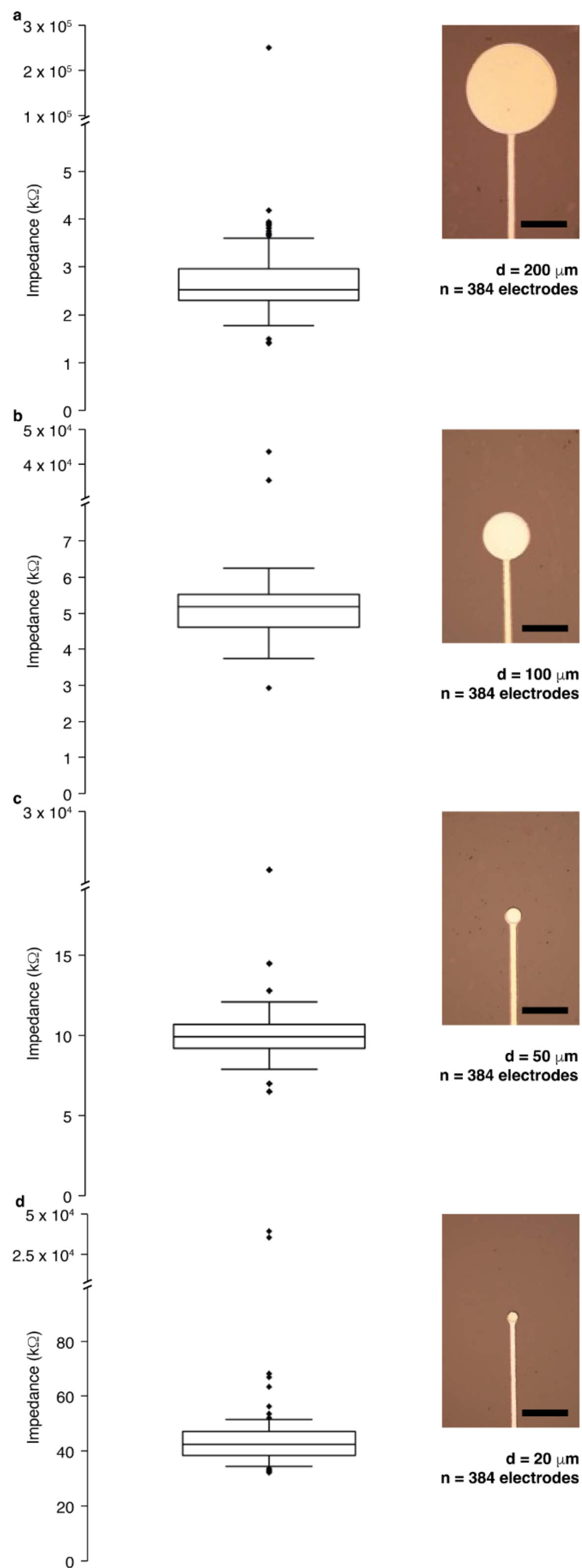

Fig.14: Variability of electrode impedances

Electrode impedances at 1 kHZ for **a**, 200 µm **b,** 100 µm **c**, 50 µm and d, 20 µm diameter electrodes. Measurements were taken from 6 wafers with 8 devices on each wafer.

in vivo Implantation

As discussed above, devices created through this protocol are often used *in vivo*. Protocols for surgical procedure development and implantation vary widely based on desired tissue placement (Fig.10)[22,42,45,46]. However, some general steps and procedures can be consistently applied throughout this process. Above, we outlined some of the basic steps for pre-operative procedures for rodent work (mouse and rat), along with some strategies for device placement in different tissues. Of note, implant design must accommodate the surgery of interest, inclusive of placement of different assistive features (suture loops, anchor pointers, fiducial markers, etc.) for any specific surgery. As such, some iteration or experience is typically required in terms of developing a device that is feasible for surgical placement.

Cost Estimation

The cost per device can vary substantially, depending on country of production, cleanroom facility fees, and mechanisms for charging. Cleanroom facilities are often set up as user facilities to accommodate the substantial cost of equipment for production. In these cases, the majority of the cost will be directed at a monthly or yearly fee with potential additional costs in hourly equipment usage. Other cleanrooms may not have user fees, in which case, the researcher is presumably responsible for purchase of chemicals and materials. Cost of materials and chemicals is relatively inexpensive, but some of the equipment used in this protocol is of substantial cost to purchase and maintain for an individual lab. Researchers intending to use this protocol should identify a nearby cleanroom facility to determine payment structure for operation of equipment in this facility when considering budgeting for this type of process.

Conclusion

In summary, this fabrication method for thin-film bioelectronic devices, featuring PEDOT:PSS electrodes and organic electrochemical transistors, offers a reproducible and versatile approach. The process allows for the fabrication of mechanically flexible implants suitable for diverse medical applications, showcasing compatibility with various tissues and addressing some of the challenges associated with conventional, stiff bioelectronic devices. The provided mask design, materials list, and step-by-step procedure offer a comprehensive guide for researchers familiar with cleanroom procedures, enabling the production of these implants within a 3-4 day timeframe. The potential applications span from interfacing with dynamic tissues like those in the gastrointestinal system to providing high-resolution recordings in the peripheral or central nervous system. The inclusion of organic electrochemical transistors in these implants extend their functionality, enabling chemical sensing for neurotransmitters and biomarkers.

Author Contributions

P.O, S.V.B, S.L.B, and A.J.B conceived and designed the study. P.O, S.V.B, S.L.B, and A.J.B designed the masks. P.O, S.V.B, and A.J.B fabricated the devices. S.L.B

performed characterisation of the OECT's and P.O performed characterisation of the electrodes, and the subsequent data analysis. A.J.B, T.H, and G.G.M supervised the study. T.H, and G.G.M acquired funding for the study and supported with administration. P.O, S.V.B, S.L.B, and A.J.B wrote the manuscript.

Acknowledgments
This work was funded by the EPSRC (EP/T004908/1, IAA Follow-on Fund RG90413) and MRC CiC (RG84584). P.O would like to acknowledge funding from the EPRSC and Johnson Matthey iCASE studentship (G102881), and the Royal Commission of the Exhibition of 1851 (G106790). A.J.B. would like to acknowledge his fellowship from the Human Frontier Science Program (HFSP) (LT000034/2020-C). S.V.B was supported by the NIHR Cambridge Biomedical Research Centre (NIHR203312). The views expressed are those of the authors and not necessarily those of the NIHR or the Department of Health and Social Care. S.V.B acknowledges the HORIZON EUROPE UKRI UNDERWRITE INNOVATE program (COPE-Nano, 10078978) and from the ECH2020 FUTURE & EMERGING TECHNOLOGIES (FET) program (MITICS, GA 964677). S.L.B. acknowledges funding from the Cambridge International & Churchill Pochobradsky Scholarship. The authors would also like to acknowledge R. Mizuta for his work in preparing Figures 1, 2, and 10.

Competing Interests
The authors declare that they have no conflict of interest.

References

1. Feigin, V. L. *et al.* Global, regional, and national burden of neurological disorders, 1990–2016: a systematic analysis for the Global Burden of Disease Study 2016. *Lancet Neurol* **18**, 459–480 (2019).
2. Kringelbach, M. L., Jenkinson, N., Owen, S. L. F. & Aziz, T. Z. Translational principles of deep brain stimulation. *Nature Reviews Neuroscience 2007 8:8* **8**, 623–635 (2007).
3. Colloca, L. *et al.* Neuropathic pain. *Nature Reviews Disease Primers 2017 3:1* **3**, 1–19 (2017).
4. Wang, W. *et al.* An Electrocorticographic Brain Interface in an Individual with Tetraplegia. *PLoS One* **8**, e55344 (2013).
5. Stacey, W. C. & Litt, B. Technology Insight: neuroengineering and epilepsy—designing devices for seizure control. *Nature Clinical Practice Neurology 2008 4:4* **4**, 190–201 (2008).
6. How a MED-EL Cochlear Implant is Made: Part 2 - The MED-EL Blog. https://blog.medel.com/technology/how-a-med-el-cochlear-implant-is-made-part-2/.
7. Veiseh, O. *et al.* Size- and shape-dependent foreign body immune response to materials implanted in rodents and non-human primates. *Nature Materials 2014 14:6* **14**, 643–651 (2015).
8. Zarzycki, M. Z. & Domitrz, I. Stimulation-induced side effects after deep brain stimulation – a systematic review. *Acta Neuropsychiatr* **32**, 57–64 (2020).

9. Khodagholy, D. *et al.* NeuroGrid: recording action potentials from the surface of the brain. *Nature Neuroscience 2015 18:2* **18**, 310–315 (2014).
10. Rivnay, J., Wang, H., Fenno, L., Deisseroth, K. & Malliaras, G. G. Next-generation probes, particles, and proteins for neural interfacing. *Sci Adv* **3**, (2017).
11. Kim, D. H. *et al.* Dissolvable films of silk fibroin for ultrathin conformal bio-integrated electronics. *Nature Materials 2010 9:6* **9**, 511–517 (2010).
12. Minev, I. R. *et al.* Electronic dura mater for long-term multimodal neural interfaces. *Science (1979)* **347**, 159–163 (2015).
13. Viventi, J. *et al.* Flexible, foldable, actively multiplexed, high-density electrode array for mapping brain activity in vivo. *Nature Neuroscience 2011 14:12* **14**, 1599–1605 (2011).
14. Hwang, S. W. *et al.* A physically transient form of silicon electronics. *Science (1979)* **337**, 1640–1644 (2012).
15. Woodington, B. J. *et al.* Electronics with shape actuation for minimally invasive spinal cord stimulation. *Sci Adv* **7**, 7833–7858 (2021).
16. Lacour, S. P., Courtine, G. & Guck, J. Materials and technologies for soft implantable neuroprostheses. *Nature Reviews Materials 2016 1:10* **1**, 1–14 (2016).
17. Khodagholy, D. *et al.* In vivo recordings of brain activity using organic transistors. *Nature Communications 2013 4:1* **4**, 1–7 (2013).
18. Someya, T., Bao, Z. & Malliaras, G. G. The rise of plastic bioelectronics. *Nature 2016 540:7633* **540**, 379–385 (2016).
19. Berggren, M. & Richter-Dahlfors, A. Organic bioelectronics. *Advanced Materials* **19**, 3201–3213 (2007).
20. Kurniawan, J. F. *et al.* An Adhesive-Integrated Stretchable Silver-Silver Chloride Electrode Array for Unobtrusive Monitoring of Gastric Neuromuscular Activity. *Adv Mater Technol* **6**, 2001229 (2021).
21. Sahasrabudhe, A. *et al.* Multifunctional microelectronic fibers enable wireless modulation of gut and brain neural circuits. *Nature Biotechnology 2023* **13**, 1–13 (2023).
22. Carnicer-Lombarte, A. *et al.* Ultraconformable cuff implants for long-term bidirectional interfacing of peripheral nerves at sub-nerve resolutions. *bioRxiv* 2023.04.14.536862 (2023) doi:10.1101/2023.04.14.536862.
23. Boys, A. J. *et al.* 3D Bioelectronics with a Remodellable Matrix for Long-Term Tissue Integration and Recording. *Advanced Materials* **35**, 2207847 (2023).
24. Rochford, A. E. *et al.* Functional neurological restoration of amputated peripheral nerve using biohybrid regenerative bioelectronics. *Sci Adv* **9**, (2023).
25. Wang, N., Yang, A., Fu, Y., Li, Y. & Yan, F. Functionalized Organic Thin Film Transistors for Biosensing. *Acc Chem Res* **52**, 277–287 (2019).
26. Liang, Y., Guo, T., Zhou, L., Offenhäusser, A. & Mayer, D. Label-Free Split Aptamer Sensor for Femtomolar Detection of Dopamine by Means of Flexible Organic Electrochemical Transistors. *Materials 2020, Vol. 13, Page 2577* **13**, 2577 (2020).
27. Tang, H., Yan, F., Lin, P., Xu, J. & Chan, H. L. W. Highly Sensitive Glucose Biosensors Based on Organic Electrochemical Transistors Using Platinum Gate Electrodes Modified with Enzyme and Nanomaterials. *Adv Funct Mater* **21**, 2264–2272 (2011).
28. Scheiblin, G. *et al.* Referenceless pH Sensor using Organic Electrochemical Transistors. *Adv Mater Technol* **2**, 1600141 (2017).

29. Sessolo, M. *et al.* Ion-Selective Organic Electrochemical Transistors. *Advanced Materials* **26**, 4803–4807 (2014).
30. Ordonez, J. S., Boehler, C., Schuettler, M. & Stieglitz, T. Improved polyimide thin-film electrodes for neural implants. *Proceedings of the Annual International Conference of the IEEE Engineering in Medicine and Biology Society, EMBS* 5134–5137 (2012) doi:10.1109/EMBC.2012.6347149.
31. Chang, T. Y. *et al.* Cell and protein compatibility of parylene-C surfaces. *Langmuir* **23**, 11718–11725 (2007).
32. Stieglitz, T., Beutel, H., Schuettler, M. & Meyer, J.-U. Micromachined, Polyimide-Based Devices for Flexible Neural Interfaces. *Biomedical Microdevices 2000 2:4* **2**, 283–294 (2000).
33. Ordonez, J. S., Boehler, C., Schuettler, M. & Stieglitz, T. Improved polyimide thin-film electrodes for neural implants. in *Proceedings of the Annual International Conference of the IEEE Engineering in Medicine and Biology Society, EMBS* 5134–5137 (2012). doi:10.1109/EMBC.2012.6347149.
34. Seung Woo Lee, Kyou Sik Min, Joonsoo Jeong, Junghoon Kim & Sung June Kim. Monolithic Encapsulation of Implantable Neuroprosthetic Devices Using Liquid Crystal Polymers. *IEEE Trans Biomed Eng* **58**, 2255–2263 (2011).
35. Kuo, J. T. W. *et al.* Novel flexible Parylene neural probe with 3D sheath structure for enhancing tissue integration. *Lab Chip* **13**, 554–561 (2013).
36. Middya, S. *et al.* Multishank Thin-Film Neural Probes and Implantation System for High-Resolution Neural Recording Applications. *Adv Electron Mater* 2200883 (2022) doi:10.1002/AELM.202200883.
37. Todeschini, M., Bastos Da Silva Fanta, A., Jensen, F., Wagner, J. B. & Han, A. Influence of Ti and Cr Adhesion Layers on Ultrathin Au Films. *ACS Appl Mater Interfaces* **9**, 37374–37385 (2017).
38. Yin, P., Liu, Y., Xiao, L. & Zhang, C. Advanced Metallic and Polymeric Coatings for Neural Interfacing: Structures, Properties and Tissue Responses. *Polymers 2021, Vol. 13, Page 2834* **13**, 2834 (2021).
39. Oldroyd, P. & Malliaras, G. Achieving long-term stability of thin-film electrodes for neurostimulation. *Acta Biomater* (2021) doi:10.1016/J.ACTBIO.2021.05.004.
40. Keefer, E. W., Botterman, B. R., Romero, M. I., Rossi, A. F. & Gross, G. W. Carbon nanotube coating improves neuronal recordings. *Nature Nanotechnology 2008 3:7* **3**, 434–439 (2008).
41. Middya, S. *et al.* Microelectrode Arrays for Simultaneous Electrophysiology and Advanced Optical Microscopy. *Advanced Science* **8**, 2004434 (2021).
42. Boys, A. J. *et al.* Implantable Bioelectronics for Real-time in vivo Recordings of Enteric Neural Activity. *bioRxiv* 2024.03.22.586292 (2024) doi:10.1101/2024.03.22.586292.
43. Han, S., Polyravas, A. G., Wustoni, S., Inal, S. & Malliaras, G. G. Integration of Organic Electrochemical Transistors with Implantable Probes. *Adv Mater Technol* **6**, 2100763 (2021).
44. Bidinger, S. L., Han, S., Malliaras, G. G. & Hasan, T. Highly stable PEDOT:PSS electrochemical transistors. *Appl Phys Lett* **120**, (2022).
45. Boys, A. J. *et al.* 3D Bioelectronics with a Remodellable Matrix for Long-Term Tissue Integration and Recording. *Advanced Materials* **35**, 2207847 (2023).
46. Woodington, B. J. *et al.* Flexible circumferential bioelectronics to enable 360-degree recording and stimulation of the spinal cord. *Sci Adv* **10**, 1230 (2024).

47. Smith, S. W. *The Scientist and Engineer's Guide to Digital Signal Processing. California Technical Pub.* (1997).
48. Halnes, G. *et al.* Electric Brain Signals: Foundations and Applications of Biophysical Modeling. *Electric Brain Signals* (2024) doi:10.1017/9781009039826.
49. Graziane, Nicholas., Dong, Yan., Zhu, Xiyu. & Grace, A. A. . Electrophysiological Analysis of Synaptic Transmission. 289 (2022) doi:10.1007/978-1-0716-2589-7.
50. He, B. *Neural Engineering: Third Edition. Neural Engineering: Third Edition* (Springer International Publishing, 2020). doi:10.1007/978-3-030-43395-6/COVER.
51. van Drongelen, W. Signal processing for neuroscientists: An introduction to the analysis of physiological signals. *Signal Processing for Neuroscientists: An Introduction to the Analysis of Physiological Signals* 1–308 (2006) doi:10.1016/B978-0-12-370867-0.X5000-1.
52. Boehler, C., Carli, S., Fadiga, L., Stieglitz, T. & Asplund, M. Tutorial: guidelines for standardized performance tests for electrodes intended for neural interfaces and bioelectronics. *Nature Protocols* vol. 15 3557–3578 Preprint at https://doi.org/10.1038/s41596-020-0389-2 (2020).
53. Schiavone, G. *et al.* Guidelines to Study and Develop Soft Electrode Systems for Neural Stimulation. *Neuron* **108**, 238–258 (2020).
54. Cogan, S. F. Neural stimulation and recording electrodes. *Annu Rev Biomed Eng* **10**, 275–309 (2008).
55. Harris, A. R., Morgan, S. J., Wallace, G. G. & Paolini, A. G. A Method for Systematic Electrochemical and Electrophysiological Evaluation of Neural Recording Electrodes. *JoVE (Journal of Visualized Experiments)* e51084 (2014) doi:10.3791/51084.
56. Bidinger, S. L. *et al.* Pulsed transistor operation enables miniaturization of electrochemical aptamer-based sensors. *Sci Adv* **8**, 4111 (2022).
57. Ohayon, D., Druet, V. & Inal, S. A guide for the characterization of organic electrochemical transistors and channel materials. *Chem Soc Rev* **52**, 1001–1023 (2023).
58. Rivnay, J. *et al.* Organic Electrochemical Transistors with Maximum Transconductance at Zero Gate Bias. *Advanced Materials* **25**, 7010–7014 (2013).
59. Friedlein, J. T., McLeod, R. R. & Rivnay, J. Device physics of organic electrochemical transistors. *Org Electron* **63**, 398–414 (2018).
60. Khodagholy, D. *et al.* High transconductance organic electrochemical transistors. *Nature Communications 2013 4:1* **4**, 1–6 (2013).
61. Rivnay, J. *et al.* Organic Electrochemical Transistors with Maximum Transconductance at Zero Gate Bias. *Advanced Materials* **25**, 7010–7014 (2013).
62. Dijk, G., Kaszas, A., Pas, J. & O'Connor, R. P. Fabrication and in vivo 2-photon microscopy validation of transparent PEDOT:PSS microelectrode arrays. *Microsystems & Nanoengineering 2022 8:1* **8**, 1–8 (2022).